Springer

KSME

Journal of Mechanical Science and Technology 30 (10) (2016) 4669~4677
www.springerlink.com/content/1738-494x(Print)/1976-3824(Online)
DOI 10.1007/s12206-016-0937-4

Evaluation of structural deformations of a mechanical connecting unit for oxidizer supplies by thermo-mechanical simulation †

Sang-Woo Kim*

Department of Mechanical Engineering, Institute of Machine Convergence Technology, Hankyong National University, Anseong-si, Gyeonggi-do 17579, Korea

(Manuscript Received February 4, 2016; Revised May 27, 2016; Accepted May 30, 2016)

Abstract

A Mechanical connecting unit (MCU) used in ground facilities for a Liquid propellant rocket (LPR) acts as a bridge between the onboard system and the ground oxidizer filling system. It should be resistant to structural deformations in order to guarantee successful supply of a cryogenic oxidizer and high pressure gases without reduction of sealing capability. The MCU consists of many components and linkages and operates under harsh conditions induced by a cryogenic oxidizer, high pressure gases and other mechanical forces. Thus, the evaluation of structural deformation of the MCU considering complex conditions is expensive and time consuming. The present study efficiently evaluates the structural deformations of the key components of the MCU by Thermo-mechanical simulation (TMS) based on the superposition principle. Deformations due to the mechanical loadings including weights, pressures, and spring forces are firstly evaluated by using a non-linear flexible body simulation module (FFlex) of Multi-body dynamics (MBD) software, RecurDyn. Then, thermal deformations for the deformed geometries obtained by RecurDyn were subsequently calculated. It was conducted by using a Finite element (FE) analysis software, ANSYS. The total deformations for the onboard plate and multi-channel plate in the connecting section due to the mechanical and thermal loadings were successfully evaluated. Moreover, the outer gaps at six points between two plates were calculated and verified by comparison to the measured data. Their values and tendencies showed a good agreement. The author concluded that the TMS using MBD software considering flexible bodies and an FE simulator can efficiently evaluate structural deformations of the MCU operating under the complex load and boundary conditions.

Keywords: Mechanical connecting unit (MCU); Liquid propellant rocket (LPR); Oxidizer; Thermo-mechanical simulation (TMS); Structural deformation

1. Introduction

A Liquid propellant rocket (LPR) uses a liquid oxidizer, kerosene fuel, and other gases to deliver a more massive payload to orbit [1, 2]. To guarantee the launch operation for the LPR, the flammable and explosive supplies should be safely delivered from the ground oxidizer filling systems to the onboard tanks in the LPR. The ground and onboard systems are mechanically connected by a Mechanical connecting unit (MCU) at their interface. The MCU plays a very important role in delivering gases and preventing leakage. Thus, it should be resistant to structural deformations in order to guarantee successful supply of a cryogenic oxidizer to the LPR.

Realistically, structural deformations of the MCU are inevitable because it operates under the harsh environment induced by a cryogenic oxidizer, high pressure gases, and the heavy weight of components. The harsh environmental conditions can cause non-uniform deformations, i.e., incompatible interfaces resulting in reduction of sealing capability. Even a small deformation of the MCU can adversely affect the delivery of a liquid oxidizer and the pressure dissipation of gases. Therefore, structural deformations of the MCU should be thoroughly estimated before operation because a leakage of explosive fluids and/or gases can lead to a catastrophic explosion [3-5].

Meanwhile, many problems of structural deformations including coupled thermal and mechanical loading conditions have been solved by the Thermo-mechanical simulation (TMS). In terms of the TMS, a variety of methodologies have been developed and used to evaluate stresses and deformations. Choi et al. [6, 7] solved coupled thermo-mechanical problems for brake disks. They performed the TMS by developing an asymmetric Finite element (FE) model to solve the contact problems of brake disks and examine their thermo-elastic instability phenomenon. Wang et al. [8] evaluated thermo-mechanical coupling stresses and deformations of a piston and its pin using commercial software, ANSYS. They also performed dynamic analysis to examine the dynamic responses and fatigue characteristics. The TMS has been often applied to simulate structural behaviors of mechanical materi-

*Corresponding author. Tel.: +82 31 670 5113, Fax.: +82 31 670 5118
E-mail address: swkim@hknu.ac.kr
† Recommended by Associate Editor Jeong Sam Han

als during manufacturing processes. Rouquette et al. [9] performed the TMS based on FE analysis to investigate the effects of temperature on the residual stress field induced by shot-peening process. Hong et al. [10] also successfully simulated the hot continuous rolling processes of large-diameter bar by the TMS based on elastoplastic FE analysis.

However, it is quite inefficient to calculate structural deformation of the MCU only using finite element analysis. Numerical estimation of structural deformations of the MCU requires complicated calculation techniques because the MCU is made up of many linkages and flexible pipes, and subjected to complex mechanical and thermal loadings. It also has complicated boundary conditions including contact conditions, spring joints and sliding constraints. Using an FE simulator considering all these complicated conditions is grossly inefficient. An FE analysis can be generally performed by simplifying the complex geometries and analysis conditions to estimate the structural deformations, which means that model reduction should be conducted. However, it is also time consuming.

Our study reduced the effort for model reduction by directly modelling the multi-components using the commercial software, RecurDyn [11-13]. This method is intuitive and able to save the time for model reduction. Then, the TMS based on the superposition principle was conducted to evaluate the structural deformations of the key components of the MCU, i.e., an onboard plate and a multi-channel plate, by using RecurDyn and commercial FE simulator, ANSYS. In details, mechanical deformations were first calculated by using a nonlinear flexible body simulation module (FFlex) of Multi-body dynamics (MBD), RecurDyn. This method to evaluate mechanical deformations can reduce calculation time even though complex geometries, loadings, and boundary conditions are considered in the calculation. The deformed profiles evaluated in the first step were subsequently imported into ANSYS. Then, thermal analysis was performed to obtain the total deformation of the plates. Moreover, the outer gaps at six points between two plates were calculated and verified by comparison to the measured data.

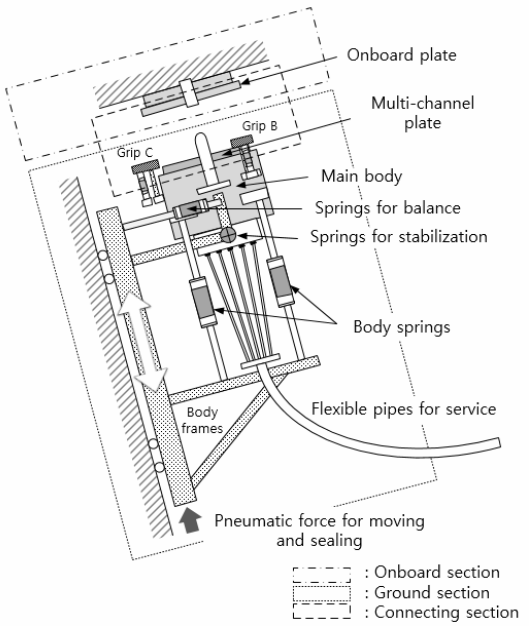

(a) Mechanical connecting unit system

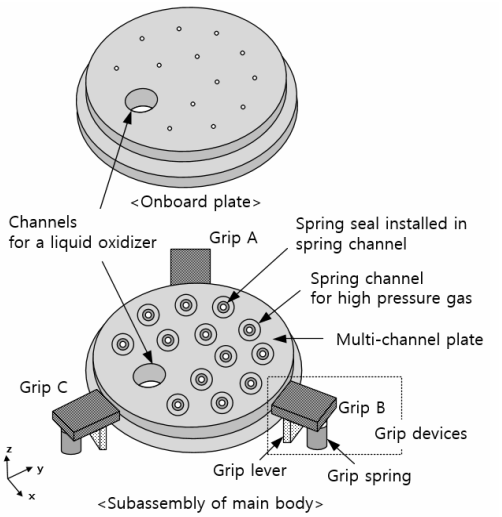

(b) Connecting section

Fig. 1. Schematic illustration of a mechanical connecting unit.

2. Mechanical connecting unit (MCU)

2.1 Configuration

The MCU is a mechanical interface device between the ground oxidizer filling systems and onboard systems. It mainly consists of three sections: The onboard section, the ground section, and the connecting section. A multi-channel plate in the ground section can be mechanically coupled with an onboard plate by three grip devices through an automatic connecting mechanism after the main body in the ground section approaches the onboard plate. Fig. 1 shows the schematic illustration of the MCU.

Several linkages and body frames were constructed to support the main body and service pipes. The springs for supporting, balancing, and stabilizing the main body are installed at several interfaces between the main body and body frames, as shown in Fig. 1(a). The number of body springs, springs for balance, and springs for stabilization are six, two and two, respectively.

The main body consists of several components, including a multi-channel plate, grip devices, grip springs, spring channels for gases, etc. They play a major role in connecting mechanisms and the supply of a cryogenic oxidizer and high pressure gases. Thirteen channels for high pressure gases are located in the multi-channel plate of the main body. A spring seal is a type of seal that use a spring force and is installed in each spring channel to secure the sealing of high pressure gases by filling the space between an onboard plate and a multi-channel plate.

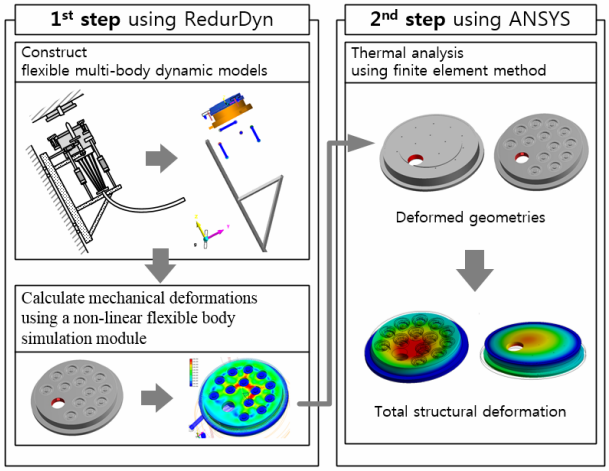

Fig. 2. Two-step analysis procedure for a thermo-mechanical simulation.

The main body and the other components of the ground parts can move up and down to couple or decouple the two plates by applying or removing pneumatic force. Three grips with 120° intervals are positioned near the edge of the multi-channel plate as shown in Fig. 1(b). These grips can rotate on the grip lever by applying pneumatic forces. Dominant grip forces are achieved by the grip springs after the grip devices have completely coupled with the onboard plate.

2.2 Operating procedure

The connecting mechanism of the MCU operates in five steps: i) A pneumatic force moves the main body and body frames to an onboard plate; ii) three grip devices are closed by applying nominal pneumatic grip forces; iii) the grip forces increase up to about 10%; iv) a liquid oxidizer and high pressure gases are supplied from ground filling systems to onboard tank systems; v) the oxidizer and gases are supplied with pneumatic forces for completion of tight sealing.

3. Thermo-mechanical simulation

3.1 Procedure of analysis

The structural deformations were investigated through TMS based on the superposition principle. It was a reasonable investigation because the interface of the MCU exhibited small variation in linear dimensions in the linear region; that is, the deformations were fully recovered after removing the external thermal and mechanical loadings.

The MCU is made up of many linkages and is subjected to complex mechanical and thermal loadings. It also has complex boundary conditions including contact conditions, spring and revolute joints, sliding constraints, etc. Our study solves complex problems using the commercial MBD software and FE simulator. Total deformations of the MCU, especially the multi-channel plates and onboard plate, were evaluated using a two-step analysis procedure, as shown in Fig. 2.

Mechanical deformations of two plates due to the complex forces and the pressure of gases were first evaluated by using a non-linear flexible body simulation module (FFlex) in RecurDyn. In the first step of the analysis, the dead weights of all components, linkages, and joints were considered. An FFlex module can calculate nonlinear deformations in a flexible body with FE meshes. It can be used in models with flexible bodies in contact with each other or for evaluating nonlinear deformation of the bodies [14]. In the FFlex module [14, 15], the Equation of motion (EOM) for multi-rigid bodies is constructed based on the virtual work principle:

$$F^r = TRS^T\left(M\ddot{r} + \left(\Phi_z^{rr}\right)^T\lambda^{rr} + \left(\Phi_z^{er}\right)^T\lambda^{er} - Q^r\right) = 0\,. \tag{1}$$

The EOM for FEs of flexible bodies is:

$$F^e = M^f\ddot{q}^f + \left(\Phi_{q^f}^{ff}\right)^T\lambda^{ff} - Q^f = 0\,. \tag{2}$$

The system equations for the MCU are derived based on the Multi-flexible body dynamics (MFBD) technology [15, 16] and relative coordinate systems by combining Eqs. (1) and (2), as below:

$$\begin{bmatrix} \frac{\partial F^f}{\partial q^f} & \frac{\partial F^f}{\partial q^r} & 0 & \left(\Phi_{q^f}^{fr}\right)^T \\ \frac{\partial F^r}{\partial q^f} & \frac{\partial F^r}{\partial q^r} & TRS^T\left(\Phi_z^{rr}\right)^T & TRS^T\left(\Phi_z^{fr}\right)^T \\ 0 & \Phi_{q^r}^{rr} & 0 & 0 \\ \Phi_{q^f}^{fr} & \Phi_{q^r}^{fr} & 0 & 0 \end{bmatrix} \begin{bmatrix} \Delta q^{ff} \\ \Delta q^{rr} \\ \Delta\lambda^{rr} \\ \Delta\lambda^{fr} \end{bmatrix}, \tag{3}$$
$$= -\begin{bmatrix} F^f \\ F^r \\ \Phi^{rr} \\ \Phi^{fr} \end{bmatrix}$$

where TRS is the transformation matrix transferring the Cartesian coordinates into relative coordinates, and M is the mass matrix. The symbols q, r, Φ, λ, and Q and F are the relative generalized coordinate, the Cartesian coordinate, the constraint equation, the Lagrange multiplier, and the force vectors, respectively. The superscript, 'r' indicates rigid body, and 'f' means the flexible nodal body.

The multi-body system, including the FE, is solved based on the MFBD system equations expressed as Eq. (3) using the single solver to achieve the complete coupling calculation of the flexible body with FEs and MBD [15, 16].

In the second step of analysis, the deformed profiles of two plates obtained in the first step were subsequently imported into an FE simulator, ANSYS. Then thermal analyses were performed to investigate the effect of thermal loadings induced by a cryogenic oxidizer. Thermal deformations for the deformed geometries were obtained, and these were the superimposed solutions of the mechanical and thermal deformations.

3.2 Flexible and multi-rigid body model

The flexible and multi-rigid body model for the MCU was constructed, as shown in Fig. 3. The main body is connected to the body frames through three types of springs, as shown in Figs. 1 and 3(a). The springs were modelled as linear springs with kinematic constraints (cylindrical constraints) in order to maintain equilibrium states and suppress dynamic instability during a short period of time of calculation step.

As shown in Fig. 3(b), two plates (a multi-channel plate and an onboard plate) were modeled as flexible bodies with 3D hexahedron dominant meshes, while the others were modeled as a rigid body. Large deformations can be expected at some of the parts where the grip forces are applied. Thus, mesh convergence tests were performed because the large deformations can affect numerical results. It was determined that the total numbers of elements for the onboard plate and the multi-channel plate are 24422 and 24243, respectively. The total number of nodes for the onboard plate is 98817, and that for the multi-channel plate is 95931. The meshed models for the two plates are illustrated in Fig. 4. Three grip devices are connected to grip springs modeled as linear springs. When the MCU is coupled, some parts of grip springs are directly contacted to the meshed onboard plate.

Thus, the "Solid to flex contact condition" was applied to the interface in order to transfer tractions from the grip devices to the onboard plate. The contact stiffness and damping coefficient are 2.0e5 N/mm and 5.0e5 Ns/mm, respectively. The edges on the upper surface of the onboard plate and on the lower surface of the multi-channel plate are fixed to the LPR and rigid main body, respectively.

The rotating joints and rotating springs were applied at the ends of grip levers. The spring seals in the spring channels were modeled as linear springs connected to the channels in the onboard plate.

3.3 Conditions used in calculations

The material properties for steel, SUS 316L, used in the multi-channel plate and onboard plate are presented in Table 1. In the first step of the analysis, the external forces, including the weights of all components, the external forces generated by the pressures of gases, and the pneumatic forces for moving the body frames were considered in the simulation. Some of the spring coefficients were tuned for suppressing the dynamic instability during the simulation. Table 2 shows the forces and spring coefficients used in the analysis.

4. Results

The structural deformations for the key components, i.e., the onboard plate and the multi-channel plate, were evaluated through a two-step analysis procedure.

Table 1. Material properties for the onboard and multi-channel plate.

Properties	Units	Values
Young's modulus	GPa	193
Poisson's ratio	mm/mm	0.3
Density	kg/m^3	8,000
Thermal conductivity	W/m/k	16.3
Specific heat	J/kg/K	500
CTE*	K^{-1}	1.6e-05
Convection coefficient	W/m^2/K	5

*CTE: Coefficient of thermal expansion

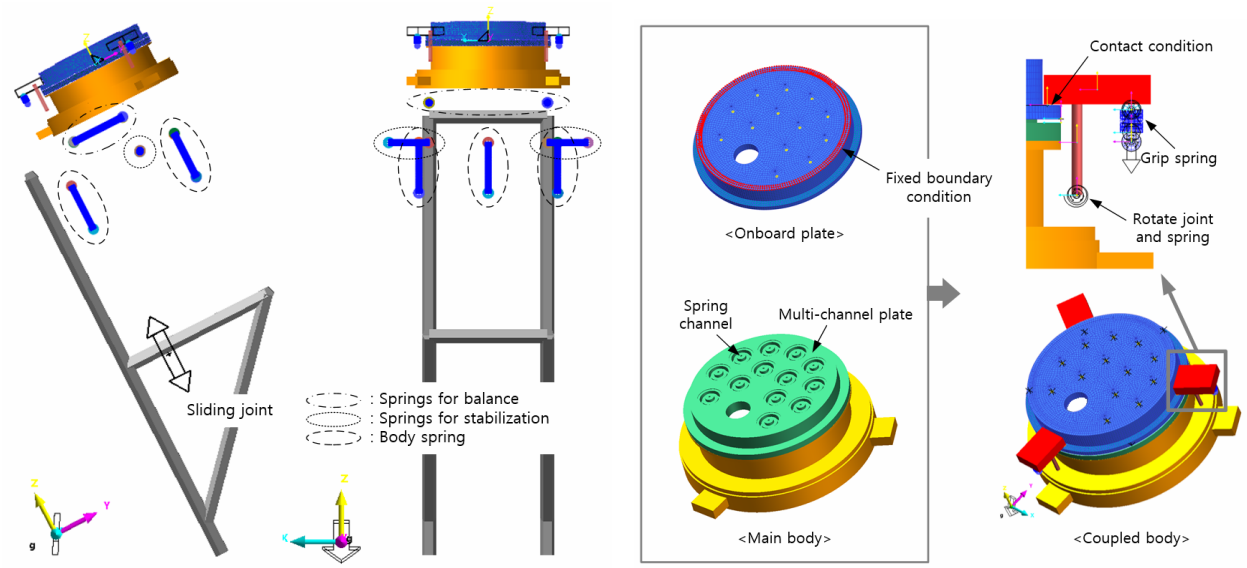

(a) Full model in RecurDyn (b) Coupled body model

Fig. 3. Flexible and multi-rigid body models in RecurDyn for a mechanical connecting unit.

Table 2. Normalized forces and spring coefficients used in the calculation.

Items		Values	Units
Weight or forces	Pneumatic force	1	N/N
	Main body with service pipes	0.325	
	Body frames with springs	0.136	
	Gas force	1.938	
Spring coefficients	Grip springs	1	Nmm / Nmm
	Springs for balance	4	
	Springs for stabilization	0.2	
	Body springs	1.6	
	Springs in gas channels	0.568	
	Rotational springs at grip springs	4.0e+8	Nmm/rad

The forces and spring coefficients used in the analysis were normalized with respect to the pneumatic force and the spring coefficient of the grip spring, respectively. Non-normalized values were used in the actual calculation.

The analysis in the first step was performed with a total time of 2.0 sec and 100 steps of simulation. In the second step of the analysis, a cryogenic oxygen temperature of -183.2˚C and a convection coefficient of 5 W/m^2/K were applied on the internal surface of the oxidizer channel and the other surfaces of the two plates, respectively. The thermal analysis was undertaken with a total calculation time of one second and a flux convergence of 1.0e-04. The CPU times for the first step and the second step of the analysis were 847 sec and 6 sec, respectively.

4.1 Calculation of mechanical deformation

The mechanical deformations were evaluated through the first step of the analysis using an MBD module with flexible bodies. Fig. 5 shows the magnitude in mm of mechanical deformations of the onboard plate and the multi-channel plate.

Local deformations of the onboard plate occurred at the interface contacted to the grip devices. The maximum deformation of 0.125 mm was observed at Grip B, and the deformations at Grip A and C were 0.117 mm and 0.122 mm, respectively. Actually, the grip springs were built by stacking the disk springs with high spring coefficients, and they produce large external forces acting on the interfaces. Mechanical deformations at these regions were relatively greater than those evaluated at any other calculation points in the plate.

The onboard plate is contacted to the multi-channel plate through the “spring seals” installed in the spring channels, as shown in Fig. 1(b).

The deformations with circular contour were observed, and their magnitude became greater when approaching the center of the plate. Thus, the onboard plate was deformed into a convex shape with the maximum deformation of 0.113 mm at the center. This tendency is reasonable since the external forces generated by the spring seals pressed the lower surface of the

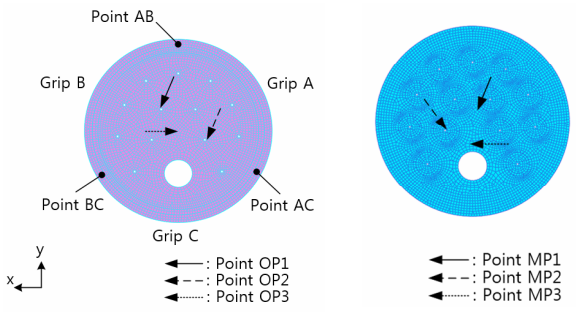

(a) Onboard plate (b) Multi-channel plate

Fig. 4. Meshed models in bottom view for flexible bodies.

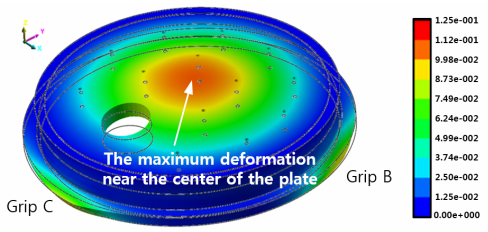

(a) Onboard plate

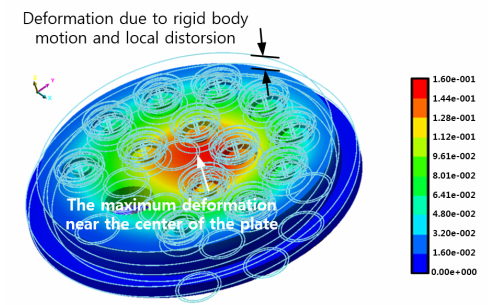

(b) Multi-channel plate

Fig. 5. Mechanical deformations of the onboard plate and the multi-channel plate.

plate in the z direction, and the grip forces did not exert forces with a large difference in magnitude and were applied on the edges of the plate at regular interval. Of course, the grip forces varied slightly from grip to grip mainly due to the tilted body frame of the MCU, but the variation was negligible to identify the results; the differences were less than 5.8% of the maximum grip force.

In the case of the multi-channel plate, the major deformations due to the grip forces were not observed, because they were not directly contacted to the grip devices. Of significance is that deformations and a rigid body motion were collocated because the multi-channel plate was not fixed on the ground or a motionless rigid body. However, the onboard plate did not globally show any rigid body motion since it was fixed on the body of the LPR, as shown in Fig. 5. The solid lines indicate the original shape, while solid parts with smooth contour are the deformed geometries. The quantity of a rigid body motion observed at the center of mass is:

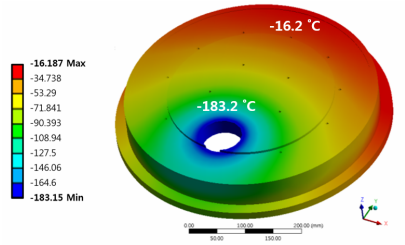

(a) Onboard plate

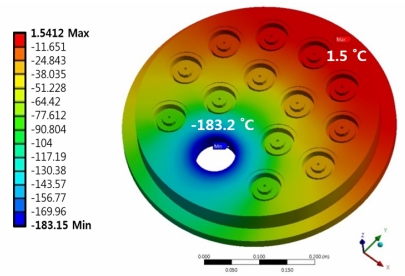

(b) Multi-channel plate

Fig. 6. Distribution of steady-state temperature for the onboard plate and multi-channel plate.

$$<\vec{x}, \vec{y}, \vec{z}, \vec{\phi}, \vec{\theta}, \vec{\psi}> = <0, -0.099, -0.770, -0.896, 0, 0>, \quad (4)$$

where $\vec{x}$, $\vec{y}$,, $\vec{z}$ (in mm) are translation motions in the direction of x, y, z, respectively.

The rotational vectors (in degrees) around the x-axis, y-axis, and z-axis are expressed as $\vec{\phi}$, $\vec{\theta}$, $\vec{\psi}$, respectively. In our study, the pure deformations of the multi-channel plate were estimated by subtracting vector quantities of rigid body motion from the movement of nodes.

However, rigid body motion was considered when the outer gaps of the plates discussed in the next chapter were estimated.

For the multi-channel plate, the maximum deformation of 0.158 mm in magnitude was observed near the center of the plate, as shown in Fig. 5(b). The deformations in the -z direction increased because the reaction forces generated by the spring seals acted on the plate in the -z direction. Thus, the plate showed a concave shape. The deformations in the z direction at Point MP1, MP2, and MP3 defined in Fig. 4(b) were -0.158 mm, -0.123 mm and -0.114 mm, respectively. The majority of deformations in the z-direction accounted for deformations in magnitude.

4.2 Coupled structural-thermal analysis

Total structural deformations as well as thermal deformations, were evaluated in the second step of the analysis using the FE simulator. A low temperature cryogenic oxygen (-183.2°C) was applied on the internal surface of the oxidizer channel in the onboard plate and the multi-channel plate. A steady-state thermal analysis, as opposed to a transient analysis, was performed because the transient responses were quickly dissipated right after supplying the oxidizer.

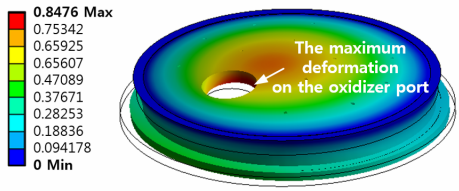

(a) Onboard plate

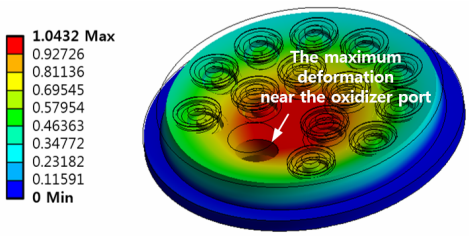

(b) Multi-channel plate

Fig. 7. Total and thermal deformations of the onboard plate and the multi-channel plate.

Fig. 6 shows the distribution of steady-state temperature for the two plates. The temperatures in the regions far from the oxidizer channel of the onboard plate and the multi-channel plate converged to -16.2°C and 1.5°C, respectively. Some parts of the plates, especially near the oxidizer channel, shrunk according to the distribution of the steady-state temperature; the maximum strains of 0.013 mm/mm and 0.007 mm/mm in contraction were estimated for the onboard plate and the multi-channel plate, respectively. Moreover, large temperature gradients were observed in proximity to the oxidizer channel.

The total structural deformations for the two plates were evaluated and depicted in Fig. 7. The solid lines represent the original shapes calculated in the first step of the analysis, and the total structural deformations are presented as deformed geometries based on the position of the nodes. The deformations due to thermal loadings were investigated and are presented as colored contours in Fig. 7.

For thermal deformations, deformations in magnitude with broad elliptic contour were observed in both plates. This is because the oxidizer channel was eccentrically positioned from the center of the plates and thermal heat was transferred to the all surface of the plates with a constant convection coefficient except for the internal surface of the oxidizer channel.

However, the shapes of the deformations of the two plates were completely different because the fixed boundary conditions were positioned at opposite sides. Therefore, the deformed geometries of the onboard plate formed a convex shape, and those of the multi-channel plate presented a concave shape. The maximum deformations in magnitude induced by thermal loadings were 0.848 mm and 1.043 mm for the onboard plate and the multi-channel plate, respectively.

Fig. 8 shows the deformations in magnitude of the two plates according to analysis steps. They were pure deformations without consideration of rigid body motion of the multi-

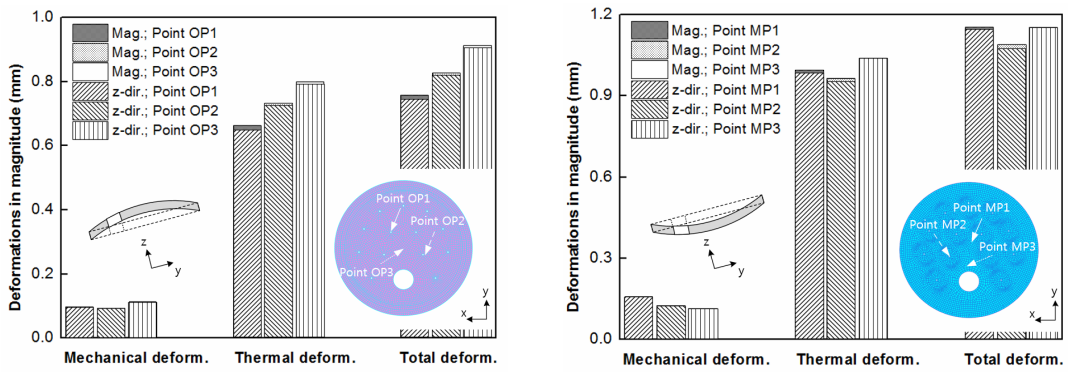

(a) Onboard plate (b) Multi-channel plate

Fig. 8. Deformations of the onboard plate and the multi-channel plate according to analysis steps.

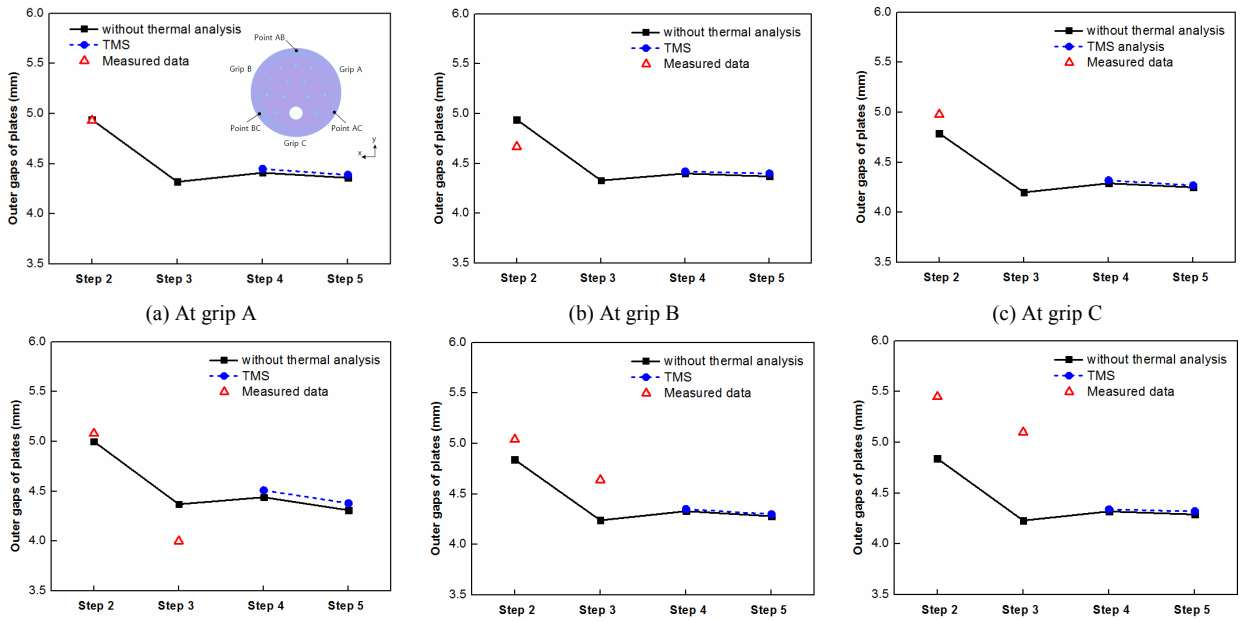

(a) At grip A (b) At grip B (c) At grip C

(d) At point AB (e) At point BC (f) At point CA

Fig. 9. Comparison of the gaps obtained from analyses and measurements.

channel plate. In both plates, it was clearly observed that the quantities of thermal deformations were greater than mechanical deformations. This indicates that mechanical robustness was more emphasized than thermal safety in the design phases.

The deformations in the z-direction accounted for most of the deformations in magnitude. For the onboard plate, the maximum value of the total deformation obtained from TMS was 0.912 mm at Point OP3, and its components were T_x = 0.010 mm, T_y = -0.104 mm, T_z = 0.906 mm.

For the multi-channel plate, the maximum value of total deformation was 1.153 mm at Point MP3, and its components were T_x = 0.003 mm, T_y = 0.010 mm, T_z = -1.153 mm. These deformations non-uniformly widen a gap in the plates resulting in the reduction of sealing. Thus, choosing the proper types of seals is important.

Our study investigated the changes of the outer gaps of two plates using TMS. The gaps were located at six points illustrated in Fig. 4 and were evaluated and verified by comparing to the measured data, as shown in Fig. 9. Investigating deformations of the components as well as rigid body motion is of primary importance to secure tight sealing of the MCU systems. Thus, a rigid body motion was incorporated into the calculation at the outer gaps.

The x-axis and y-axis on Fig. 9 indicate the operating steps of the MCU, mentioned above in Sec. 2.2, and the outer gaps between the two plates, respectively. The gaps for grip A, B, and C were only measured in the second step of the operation; that is, they were obtained after connecting the plates by three grip devices. The outer gaps for points AB, BC, and CA were also measured in the second step of the operation and addi-

tionally obtained in the third step of the operation, specifically after increasing the grip forces by up to about 10%.

At all points, the gaps dramatically decreased by about 6.4-21.3% in both analyses and measurements as the grip forces increased. Generally, the calculated gaps and their tendencies were in close agreement. Their absolute errors were less than 9.3% except for at point CA. In the case of the points BC and CA, the gaps were underestimated and the maximum error was 17.1%. This was because the exact position of the center of weight of the service pipes was not incorporated into the simulation. Actually, it was difficult to estimate the exact position of the service pipes since they are flexible. However, if we consider the more exact position moved to the -y direction, as shown in Fig. 3(a), the moments forcing the plates to rotate around the z-axis will become greater. Thus, it is expected that the errors at all points will decrease.

In the fourth step of the operation, the gaps at all points slightly increased primarily due to the internal forces acting on the gas channels induced by high pressure gases. Of particular interest is that the effect of the cryogenic oxidizer was insignificant to change the outer gaps while it became dominant in approaching the center of the plates as shown in Fig. 8. These results indicate that there are limits to achieving the completion of tight sealing by only applying the external grip forces using the grip devices. Therefore, the proper seals need to be installed between the two plates. In addition, the capacity of the seals should cover the complex mechanical and thermal deformations of the upper and lower surfaces of the plates in order to protect from leakage. In the fifth step of the operation, the gaps slightly decreased as the pneumatic forces were applied for the tight sealing of the MCU systems.

5. Conclusions

The structural deformations of the key components of the MCU (i.e., an onboard plate and a multi-channel plate) were evaluated through the TMS based on the superposition principle. The non-negligible deformations of the plates that are detrimental to the sealing of the MCU system were generated by the complex mechanical and thermal loadings. Significant deformations on the upper and lower surfaces of the plates, especially near the center and the oxidizer channel, were observed. Moreover, the quantities of thermal deformations were much greater than those of mechanical deformation. This means that the selection of the proper seals to be installed between the two plates is as important as the determination of the level of grip forces. Thus, the deformation evaluated in our study can be a guideline for determining the proper seals and to check the level of grip forces required to successfully couple the interface plates.

In addition, the changes of the outer gaps of the two plates were calculated and verified by comparison to the measured data. The calculated gaps and their tendencies generally showed a good agreement. Therefore, it was concluded that the TMS using not only MBD software considering flexible bodies but also FE simulators can efficiently evaluate structural deformations of the MCU operating under complex load and boundary conditions.

Acknowledgment

Special thanks to Dr. B. Kim, principal researcher, D. Kim, senior researcher, H. Oh, and researcher, S. Yang for their support and assistance.

References

[1] D. K. Huzel and D. H. Huang, Modern engineering for design of liquid-propellant rocket engines, *AIAA*, 147 (1992).

[2] G. P. Sutton, History of liquid propellant rocket engines in the United States, *Journal of Propulsion and Power*, 19 (6) (2003) 978-1007.

[3] T. J. Sullivan, *A review of ARAC's Involvement in the Titan II missile accident*, UCRL-85933, Lawrence Livermore National Laboratory, Livermore (1981).

[4] M. H. Dickerson and T. J. Sullivan, *ARAC Response to the Chernobyl Reactor Accident, UCRL-20834*, Livermore National Laboratory, Livermore (1986).

[5] L. E. Brownell, M. A. Farvar, G. L. Gyorey and M. York, Investigation of large scale use of radioactive krypton-85 for leak detection in the Saturn Space Vehicle, *Nuclear Structural Engineering*, 1 (1965) 492-499.

[6] C. H. Choi and I. Lee, Transient thermoelastic analysis of disk brake in frictional contact, *Journal of Thermal Stresses*, 26 (2003) 223-244.

[7] C. H. Choi and I. Lee, Finite element analysis of transient thermoelastic behaviors in disk brakes, *Wear*, 257 (2004) 47-58.

[8] Y. Wang, Y. Liu and H. Shi, Simulation and analysis of thermo-mechanical coupling load and mechanical dynamic load for a piston, *Computer Modeling and Simulation, ICCMS'10 Second International conference on*, 22-24 Jan., Sanya, Hainan, China (2010).

[9] S. Rouquette, E. Rouhaud, M. Francois, A. Roos and J. L. Chaboche, Coupled thermo-mechanical simulations of shot impacts: Effects of the temperature on the residual stress field due to shot-peening, *Journal of Materials Processing Technology*, 209 (2009) 3879-3886.

[10] H. Hong, Y. Kang, C. Feng and X. Chen, Three-dimensional thermo-mechanical coupled FEM simulation for hot continuous rolling of large-diameter mandrel bar, *Journal of Materials Science and Technology*, 19 (2003) 228-230.

[11] B. H. Lu, Y. Zhang, B. Z. Qu, J. S. Huang and Y. Liu, Research on recurdyn based simulation method for the brake shoe eccentric wear in railway freight cars, *Key Engineering Materials*, 522 (2012) 467-471.

[12] Z. Jiang and C. Zhang, Flexible multibody simulation approach in the analysis of friction winder, *Advanced Materials Research*, 97-101 (2010) 2594-2597.

[13] C. G. Yu, L. Shen and D. W. Ma, Study on simulation for

rigid-flexible coupling launch dynamics of naval gun, *Journal of System Simulation*, 23 (2009).
[14] C. Briggs and B. A. Ross, Application of integrated aero-mechanical tools to design of a flap drive system, *51st AIAA/ASME/ASCE/AHS/ASC Structures, Structural Dynamics, and Materials Conference*, 12-15 April, Orlando, Florida, USA (2010).
[15] Function Bay, *RecurDyn/Solver Theoretical Manual* (2014).
[16] X. J. Jiao, J. W. Zhang and B. B. Peng, *RecurDyn multibody system optimization and simulation technology*, Beijing: Tsinghua Publishing House (2010).

Sang-Woo Kim obtained the Ph.D. degree in Aerospace Engineering from KAIST in 2014. He was a Senior Researcher working in KARI from 2013 to 2015. He is currently an Assistant Professor in department of mechanical engineering, Hankyong National University. His interests span from the structural health monitoring (SHM) for composite structures using optical fiber sensors to the mechanical design for ground facilities of space launch vehicles.